Studies of the Inner Reorganization Energies of the Cation Radicals of 1,4-Bis(dimethylamino)benzene, 9,10-Bis(dimethylamino)anthracene, and 3,6-Bis(dimethylamino)durene by Photoelectron Spectroscopy and Reinterpretation of the Mechanism of the Electrochemical Oxidation of the Parent Diamines

Nadine E. Gruhn, Norma A. Macías-Ruvalcaba, and Dennis H. Evans*

Department of Chemistry, University of Arizona, Tucson, Arizona 85721

Received: January 22, 2006; In Final Form: March 10, 2006

The inner reorganization energy of the cation radical of 1,4-bis(dimethylamino)benzene, **1**, has been determined to be 0.72 ± 0.02 eV by means of gas-phase photoelectron spectroscopy (PES). PES studies of 9,10-bis-(dimethylamino)anthracene, **2**, and 3,6-bis(dimethylamino)durene, **3**, demonstrate that their reorganization energies are smaller than that of **1**. The effect of lowering the inner reorganization energy on the rate constant for an electrochemical electron-transfer reaction is to increase the electron-transfer rate constant, k_s. However, voltammetric studies of the two-electron oxidation of **2** and **3** indicate that the values of k_s for each step are smaller than those for **1**, in contradistinction to the measured differences in reorganization energies. The voltammetric studies of **2** and **3** were reinterpreted according to a mechanism in which each step of oxidation was written as a two-step process, electron transfer with a small inner reorganization energy plus a chemical step of structural change. The agreement of simulations according to this mechanism with the experimental data was excellent. The new reaction scheme eliminated some suspicious features previously obtained with an analysis where electron transfer and structural change were considered to be concerted. In particular, all electron-transfer coefficients (α) were close to one-half, whereas the earlier treatment produced values of α much larger or smaller than one-half.

1. Introduction

Studies of the electrochemical oxidation of 1,4-bis(dimethylamino)benzene, **1**, 9,10-bis(dimethylamino)anthracene, **2**, and 3,6-bis(dimethylamino)durene, **3**, have been reported.[1] Compound **1** behaves in a completely normal fashion, showing two reversible one-electron oxidation steps to form the stable cation radical and dication. Compounds **2** and **3** show significantly different electrochemical behavior. There are two principal differences. First, cyclic voltammograms of **2** and **3** show only one two-electron oxidation peak and one two-electron reduction peak. That is, the two separate one-electron processes observed with **1** have been replaced by a single two-electron reaction. The results were previously interpreted as being an example of potential inversion, in which the removal of the second electron from **2** and **3** occurs with greater ease than removal of the first. The causes of potential inversion are the significant structural changes that accompany the oxidation reactions. These conclusions remain solid up to this date.

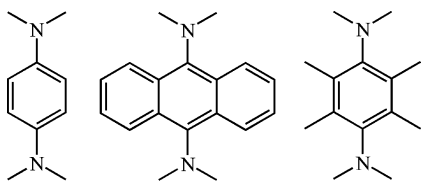

1 **2** **3**

The second difference is that the standard heterogeneous electron-transfer rate constants for the two steps of oxidation of **2** and **3** were several orders of magnitude smaller than seen for **1**. The claim was advanced that the structural changes underlying potential inversion were also responsible for much larger inner reorganization energies for **2** and **3** compared to **1** where the internal structures of the neutral, cation radical, and dication are quite similar. Therefore, the electrochemical kinetics were interpreted in terms of a concerted electron-transfer/structural-change process with a large inner reorganization energy.[1] Appropriately large reorganization energies were calculated based on the large structural changes that were found from AM1 calculations.

An alternative, recognized in the earlier work,[1] was that the electron-transfer reactions were actually two-step processes, e.g., electron transfer followed by structural change. To distinguish these two possibilities, concerted vs two-step reactions, an independent assessment of the inner reorganization energy is necessary.

It has recently been demonstrated that it is possible to obtain inner reorganization energies of cations formed from isolated neutral molecules by gas-phase photoelectron spectroscopy (PES).[2] PES directly measures the transition from the neutral state to the cation state as the vertical ionization energy, and the shape and/or vibrational structure of the ionization band give information on the cation inner reorganization energy, $\lambda^{\bullet+}$. Compared to other experimental methods used to analyze reorganization energies, gas-phase photoelectron spectroscopy has the advantage of allowing direct measure of the inner reorganization energy without contribution from solvent or other environment factors.

In the present work, we have studied **1**−**3** by PES and have determined a quantitative inner reorganization energy of 0.72

* To whom correspondence should be addressed. E-mail: dhevans@email.arizona.edu.

10.1021/jp060453b CCC: $33.50
Published on Web 04/07/2006

$\pm$ 0.02 eV for $\mathbf{1}^+$. A complete band-shape analysis of the spectra of **2** and **3** was not possible, but a qualitative conclusion was unavoidable: the inner reorganization energies of the cations of **2** and **3** must be smaller than, not larger than, that of **1** for the cation radical/neutral process.

So it is clear that the more sluggish electron-transfer kinetics of **2** and **3** compared to **1** cannot be ascribed to larger reorganization energies. The only viable alternative is to assume that the reactions are not electron transfers concerted with structural change, but that they must be two-step reactions, electron transfer followed by structural change. In the present work, new voltammetric measurements were obtained for **2** and **3** and the results were successfully analyzed in terms of two-step reactions as opposed to the concerted electron-transfer/structural-change reactions postulated earlier.

2. Experimental Section

2.1. Chemicals and Reagents. Anhydrous acetonitrile (AN, Aldrich 99.8%, <0.001% H_2O) was used as received and transferred via syringe under nitrogen. Tetrabutylammonium hexafluorophosphate (Bu_4NPF_6, Fluka) was recrystallized three times from absolute ethanol and dried in a vacuum oven at 100 °C for 24 h before use. 1,4-Bis(dimethylamino)benzene (or *N*,*N*,*N*′,*N*′-tetramethyl-*p*-phenylenediamine) was obtained from Aldrich and used as received. 9,10-Bis(dimethylamino)anthracene, **2**, and 3,6-bis(dimethylamino)durene, **3**, were prepared as described earlier.[1] Nitrogen, presaturated with solvent, was used as the purge gas.

2.2. Photoelectron Spectroscopy. Gas-phase He I photoelectron spectra were recorded using an instrument that features a 36-cm hemispherical analyzer[3a] and custom designed photon source, sample cells, and detection and control electronics.[3b] The ionization energy scale was calibrated using the $^2P_{3/2}$ ionization of argon (15.759 eV) and the $^2E_{1/2}$ ionization of methyl iodide (9.538 eV). The argon $^2P_{3/2}$ ionization also was used as an internal calibration lock of the absolute ionization energy to control spectrometer drift throughout data collection. During data collection the instrument resolution, measured using the full-width-at-half-maximum of the argon $^2P_{3/2}$ ionization, was 0.016−0.021 eV.

The samples of **1** and **3** sublimed cleanly with no visible changes in the spectra during data collection. The sample of **2** had some anthraquinone present, which was more volatile than **2**, and the spectrum reported of **2** was collected after ionizations from this contaminant were no longer present. Data was collected in a sublimation temperature range (in °C, at 10^{-4} Torr) of 23−25 for **1**, 75−90 for **2**, and 25−27 for **3** (temperatures were monitored using a "K" type thermocouple passed through a vacuum feedthrough and attached directly to the ionization cell).

The first ionization band of **1** was represented analytically with the best fit of symmetric Gaussian functions. The vertical length of each data mark in the spectra represents the experimental variance of that point. The fitting procedures are described elsewhere.[3c] A minimum number of Gaussian peaks and variable parameters were used to obtain a reasonable statistical model of an ionization band intensity contour. The Gaussians were constrained to have the same widths because all are associated with similar electronic states. The relative integrated peak areas are known within 5−10% confidence limits. Because of electron scatter, the major source of uncertainty was the determination of the base line, which was assumed to be linear over the small energy range of the first ionization band in these spectra.

The reorganization energy analysis of photoelectron spectra has been described in detail previously.[3d]

2.3. Electrochemical Cells, Electrodes, and Instrumentation. All electrochemical experiments were performed using an EG&G Princeton Applied Research Potentiostat/Galvanostat, model 283, using a standard, jacketed three-electrode cell (10 mL). The experiments were conducted at 298 K using a circulating water bath. The working electrode was a nominally 0.3-cm diameter glassy carbon disk electrode, a platinum wire served as auxiliary electrode, and the reference electrode was an Ag/Ag^+ electrode (a silver wire immersed in 0.10 M Bu_4NPF_6/0.01 M silver nitrate/acetonitrile). The reference electrode was separated from the test solution by a porous Vycor frit (Bioanalytical Systems). The potential of the silver reference electrode was periodically measured vs the potential of the ferrocenium/ferrocene couple in the solvent being studied, and all potentials are reported vs ferrocene. The highly polished glassy carbon electrode was repolished before use with 0.05-μm alumina paste (Buhler), rinsed with water, and sonicated for 5 min in water. It was then rinsed with acetone and dried with a tissue. The area of the electrode was determined to be 0.0814 cm^2 based on simulations of voltammograms of known concentrations of ferrocene in acetonitrile at 298 K using the consensus value of 2.5×10^{-5} cm^2/s for the diffusion coefficient of ferrocene.[4] The solution resistance, R_u, was almost completely compensated via *IR* compensation through positive feedback. The residual R_u was included in the simulations of the voltammograms.[5]

2.4. Calculations. Digital simulations were conducted using DigiSim from Bioanalytical Systems, version 3.03, or DigiElch, version 2.0, a free software package for the digital simulation of common electrochemical experiments (http://www.digielch-.de).[6]

Complete geometry optimization and frequency calculations were performed according to the density functional theory (DFT) using the B3LYP/6-31G(d,p) level with the Gaussian 03 program.[7] For the radical cations, the corresponding unrestricted (UB3LYP) method was used.

3. Results and Discussion

3.1. Photoelectron Spectroscopy of 1−3 and the Determination of the Inner Reorganization Energy of 1. The gas-phase valence photoelectron spectra of **1**−**3** are shown in Figure 1. For all three of these molecules, the ionizations at lower than about 10.5 eV are associated with removal of an electron from orbitals of principally arene π and/or nitrogen lone pair character. For **1** (Figure 1A), there are four ionization features observed in this lower energy region. These four ionizations of **1** are associated with the molecular orbitals formed by the symmetry-allowed combinations of the symmetric and antisymmetric combination of N lone pairs and the two arene π orbitals that evolve from the benzene π orbitals of e_{2g} symmetry. For **3** (Figure 1B), four ionizations are again observed, but because the steric encumbrance forced by the methyl groups on the durene ring twists the nitrogen lone pairs toward the plane of the arene, much less electronic communication between the nitrogen lone pairs and arene π systems occurs, so the observed ionizations are not spread over as large an energy range as observed for **1**. Rather, all four of these ionizations of **3** are located under the single band centered at about 7.8 eV. Note that while **3** might be anticipated to be easier to ionize than **1** due to the electron releasing properties of the four methyl substituents, the steric effects cause the ionization energy of **3** to actually be nearly a full electronvolt higher than that of **1**.

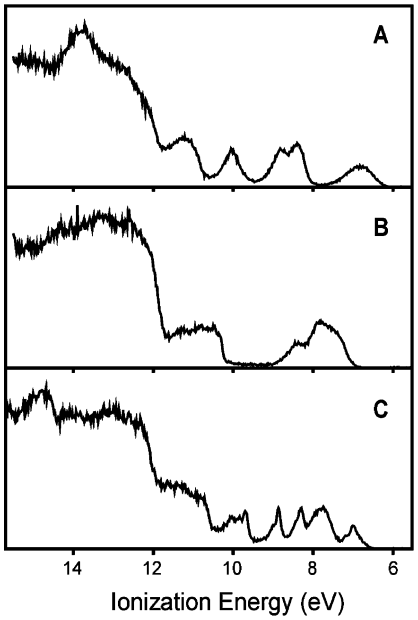

Figure 1. Gas-phase photoelectron spectra of the valence ionizations of (A) 1,4-bis(dimethylamino)benzene, **1**; (B) 3,6-bis(dimethylamino)-durene, **3**; and (C) 9,10-bis(dimethylamino)anthracene, **2**.

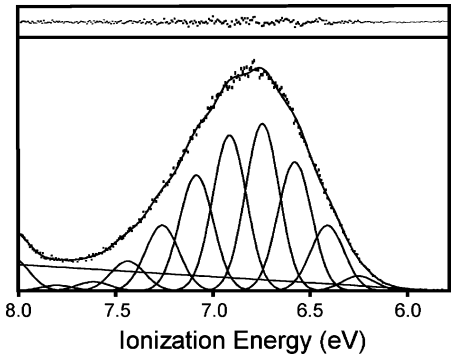

Figure 2. Gas-phase photoelectron spectrum of the first ionization of 1,4-bis(dimethylamino)benzene, **1**. The ionization band shape is modeled with a fit using a series of Gaussian functions with a spacing of 0.17 eV (1400 cm^{-1}); the residual-of-fit is shown at the top of the figure.

The spectrum of **2** (Figure 1C) contains additional ionization features due to the additional occupied orbitals of the anthracene π system.

A close-up of the first ionization band of **1** is shown in Figure 2; this band does show some partially resolved vibrational structure that is modeled with a series of Gaussians. The spacing of the Gaussians shown in this figure is 0.17 eV ($\approx$1400 cm^{-1}), which is in the energy region expected for vibrational modes associated with the C−N bonds of an arylamine. Using a harmonic oscillator model, the relative intensities of vibrational components under an ionization band should be related by a Poisson distribution that can be evaluated in terms of a unitless distortion parameter, *S*,[8a] and, indeed, the intensities of the Gaussians shown can be related by a Poisson distribution with an *S* value of 3.75. Multiplying the vibrational spacing frequency ($h\nu$) by *S* gives a quantum mechanical contribution to the reorganization energy (λ^{QM}).[8a] Any unresolved low-frequency modes, if present, result in the width of the Gaussians used to model the individual vibrational components. After taking into account the width of these Guassians that is caused by instrumental line broadening, these low-frequency modes can be treated semiclassically to give a contribution λ^{SC}.[8a] Of course, the vibrational structure observed is most likely the result of many vibrational modes rather than one particular mode, but the regular spacing of Gaussians achieved in this fit can be used to represent an average of many vibrational contributions by mode averaging.[8b−d] Alternative analytical models of the ionization intensity were also investigated to estimate the confidence levels of the reorganization energy determined from the experimental data. Setting different widths and spacings of the vibrational components besides those shown in Figure 2 can also yield reasonable models of the ionization profile with different intensities; for example, data from a fit using a Gaussian spacing of 0.12 eV ($\approx$960 cm^{-1}), which is the frequency expected for aryl ring-breathing modes, is also listed in Table 1. However, note that modeling the structure with this smaller frequency gives a proportionately larger *S* value, and the product of this smaller frequency spacing and larger *S* value then gives nearly the same value of λ^{QM}. Different models of the bandwidths contribute to uncertainty in the semiclassical contribution, but because this contribution is only a small portion of the total reorganization energy, it has little effect. The two analyses that were performed give essentially the same value for an inner reorganization energy, considering the confidence limits of the data collection and analysis, and taken together allow us to assign an inner reorganization energy of 0.72 $\pm$ 0.02 eV.

TABLE 1: Comparison of Two Separate Quantitative Analyses of the Reorganization Energy from the Photoelectron Spectrum of 1,4-Bis(dimethylamino)benzene, 1[a]

$h\nu$	*S*	λ^{QM}	λ^{SC}	$\lambda^{\bullet+}$
0.17	3.75	0.64	0.10	0.74
0.12	5.49	0.66	0.04	0.70

[a] All energy values in eV.

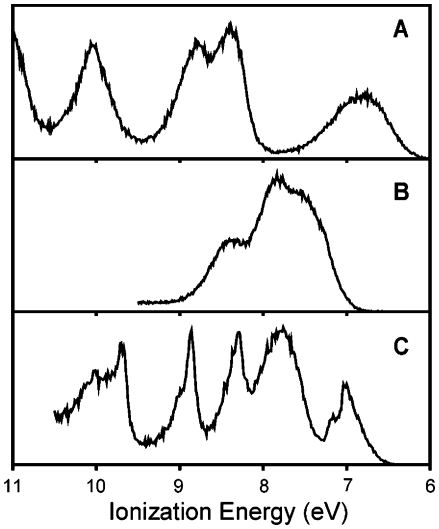

Figure 3. Comparison of the lowest ionization energy regions of the photoelectron spectra of (A) 1,4-bis(dimethylamino)benzene, **1**; (B) 3,6-bis(dimethylamino)durene, **3**; and (C) 9,10-bis(dimethylamino)anthracene, **2**.

For several reasons a quantitative analyses of the inner reorganization energies of **2** or **3** is not possible; however, a qualitative result from simple visual comparison of the widths of the first ionization features can be reached (Figure 3). As explained previously, the first ionization band of **3** is under the same band structure as the next three ionizations, so it is not possible to quantitatively analyze the shape of this band. However, considering that the overall width of the first ionization of **1** is nearly as wide as the entire band that contains these four ionizations for **3**, it is obvious that the first ionization

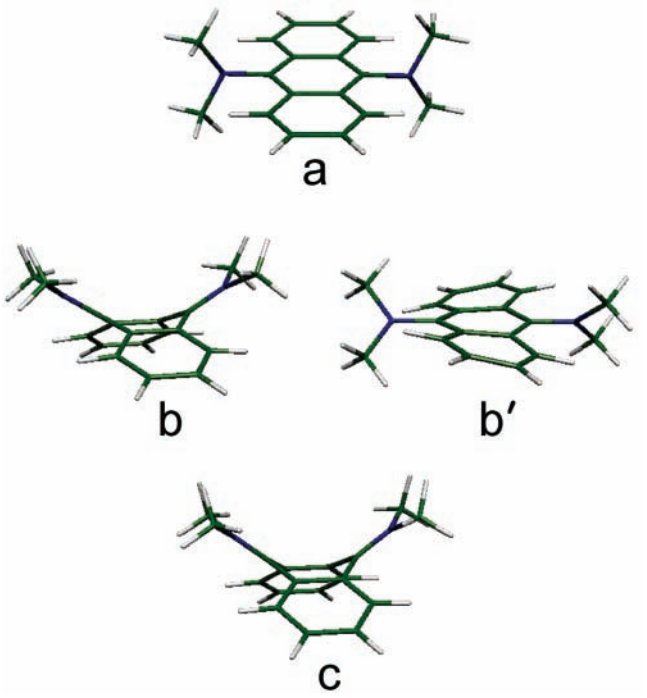

Figure 4. Optimized structures of neutral (a), cation radical (b and b′), and dication (c) of 9,10-bis(dimethylamino)anthracene, **2**.

of **3** must be more narrow than that of **1**. The shape of the first ionization band of **2** is complex and cannot be modeled with a Poisson distribution, but again the band can be visually observed to be more narrow than that of **1**. The inner reorganization energies of **2** and **3** must therefore be smaller than that of **1**.

3.2. Computation of Structures of Neutral, Cation Radical, and Dication of 2 and 3. The results of DFT calculations show for both **2** and **3** that the neutral species possesses an undistorted ring system with the dimethylamino groups, pyramidal at nitrogen, turned out of the plane of the ring system (illustrated for **2** in structure a, Figure 4). Two isomers of the cation radical were identified, one with the dimethylamino groups partially turned into the plane of the ring system with resulting distortion of the ring system (b′). The second form involved a folding of the molecule to create a boat form in the ring (central ring of **2**) with the two planar dimethylamino groups on the same side of the molecule (b). The structure of the dications was similar to the latter form of the cation radical but with a more severe folding (c).

In earlier calculations by AM1,[1] only the second, folded form of the cation radical was identified. The first form, newly discovered here, is suggested to be the relaxed form of the cations formed by PES.

3.3. Cyclic Voltammetry of 2 and 3. Data were obtained in acetonitrile containing 0.10 M Bu_4NPF_6 at scan rates of 0.1, 0.2, 0.3, 0.5, 1, 2, 3, 5, 10, 20, and 30 V/s at a glassy carbon working electrode at 298 K. The background current obtained in the absence of **2** or **3** was subtracted from the experimental voltammograms before analysis. The effects of solution resistance were compensated by positive feedback to the extent of 120 Ω, and the residual uncompensated resistance (10 Ω) was included in the simulations. One representative voltammogram of each compound is given in Figures 5 and 6, and the complete set of simulations compared to data is given in the Supporting Information.

Interpretation of the voltammetric data will be discussed in terms of the conjoined square schemes shown in Scheme 1. Here N, CR, and DC denote structures of the neutral, cation

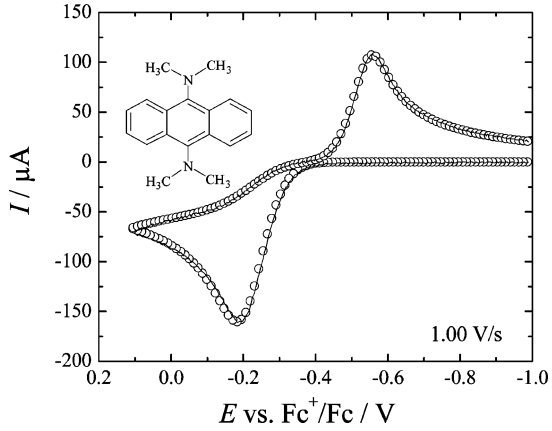

Figure 5. Cyclic voltammogram of 1.34 mM 9,10-bis(dimethylamino)-anthracene, **2**, at a glassy carbon electrode in acetonitrile containing 0.10 tetrabutylammonium hexafluorophosphate. Scan rate: 1.00 V/s. Temperature: 298 K. Full curve: background-corrected experimental voltammogram. Symbols: simulation using parameters given in Table 1.

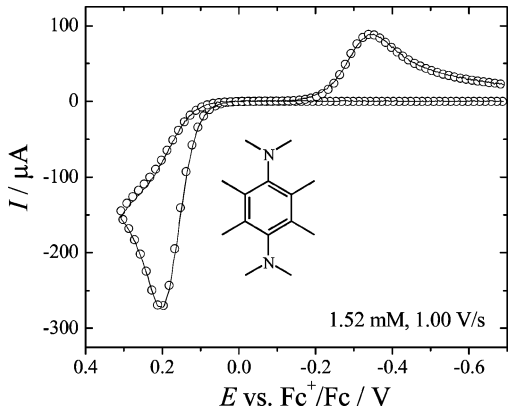

Figure 6. Cyclic voltammogram of 1.52 mM 3,6-bis(dimethylamino)-durene, **3**. Other conditions as in Figure 5.

SCHEME 1

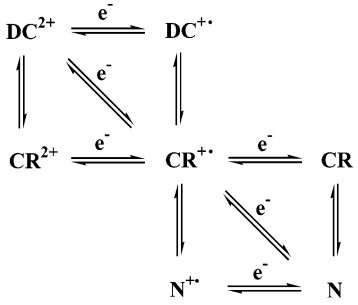

radical, and dication, respectively, and the charge, if any, is given in the superscript. Thus, $N^{+\bullet}$ indicates a cation radical with structure very similar to the equilibrium neutral structure whereas $CR^{+\bullet}$ is the cation radical in its equilibrium structure. The chemical reactions (conformational changes or isomerizations) are shown by the vertical arrows, and the parameters of each are listed in Table 3: equilibrium constants, K_j, equilibrium concentrations, c_k, and rate constants, k_l. Electrode reactions are shown by horizontal and diagonal arrows, and their parameters are also listed: formal potentials, $E°_m$, standard rate constants, $k_{s,m}$, and electron-transfer coefficients, α_m. As in any square scheme, the formal potentials and equilibrium constants are interrelated. Once values for the parameters of three sides of a square have been assigned, the value of the parameter of the fourth is defined by thermodynamics. Similarly, for a

TABLE 2: Parameters Used in Simulations[a]

parameter	9,10-bis(dimethylamino)-anthracene, **2**		3,6-bis(dimethylamino)-durene, **3**	
Analysis According to Two One-Step Electron Transfers (Ref 1)				
$E°_{CR^+/N}$	−0.26 V	−0.222 V[b]	0.06 V	0.173 V[b]
$k_{s,CR^+/N}$	0.0054 cm/s		0.0011 cm/s	
$\alpha_{CR^+/N}$	0.40		0.20	
$E°_{DC^{2+}/CR^+}$	−0.46 V	−0.552 V[b]	−0.14 V	−0.248 V[b]
$k_{s,DC^{2+}/CR^+}$	0.0011 cm/s		0.00029 cm/s	
α_{DC^{2+}/CR^+}	0.85		0.70	
$E°_{overall}$[c]	−0.36 V	−0.387 V[b]	−0.04 V	−0.038 V[b]
Analysis According to Scheme 1[d]				
$K_{CR/N}$	4.3×10^{-6}		1.4×10^{-8}	
$k_{N\rightarrow CR}$	$4\ s^{-1}$		$1.4 \times 10^{-5}\ s^{-1}$	
$k_{CR\rightarrow N}$	$9.3 \times 10^{-5}\ s^{-1}$		$1.0 \times 10^{3}\ s^{-1}$	
K_{CR^+/N^+}	3.1×10^{3}		130	
$k_{N^+\rightarrow CR^+}$	$9.2 \times 10^{9}\ s^{-1}$		$5.6 \times 10^{5}\ s^{-1}$	
$k_{CR^+\rightarrow N^+}$	$2.9 \times 10^{6}\ s^{-1}$		$4.3 \times 10^{3}\ s^{-1}$	
K_{DC^+/CR^+}	3.2×10^{-7}		7.9×10^{-5}	
$k_{CR^+\rightarrow DC^+}$	$9.7 \times 10^{3}\ s^{-1}$		$3.7 \times 10^{4}\ s^{-1}$	
$k_{DC^+\rightarrow CR^+}$	$3.5 \times 10^{6}\ s^{-1}$		$4.7 \times 10^{8}\ s^{-1}$	
$K_{DC^{2+}/CR^{2+}}$	18		3.4×10^{3}	
$k_{CR^{2+}\rightarrow DC^{2+}}$	$4.1 \times 10^{9}\ s^{-1}$		$5.8 \times 10^{4}\ s^{-1}$	
$k_{DC^{2+}\rightarrow CR^{2+}}$	$2.2 \times 10^{8}\ s^{-1}$		$17\ s^{-1}$	
$E°_{DC^{2+}/DC^+}$	−0.702 V		−0.491 V	
$k_{s,DC^{2+}/DC^+}$	14 cm/s		0.67 cm/s	
$E°_{CR^{2+}/CR^+}$	−0.476 V		−0.040 V	
$k_{s,CR^{2+}/CR^+}$	0.10 cm/s		0.026 cm/s	
$E°_{CR^+/CR}$	−0.540 V		−0.292 V	
$k_{s,CR^+/CR}$	0.024 cm/s		1.4 cm/s	
$E°_{N^+/N}$	−0.016 V		0.298 V	
$k_{s,N^+/N}$	1.2 cm/s		1.2 cm/s	

[a] Potentials are referred to the formal potential of the ferrocenium/ferrocene couple. [b] Values calculated from formal potentials and equilibrium constants from analysis according to Scheme 1 (see lower part of table). [c] The overall formal potential for the two-electron oxidation which is the average of the individual formal potentials of each step. [d] Values of all transfer coefficients were 0.5 except for $\alpha_{N^+/N}$, which was slightly smaller, 0.47.

triangle, only values of the parameters of two sides can be freely adjusted. Once they have been assigned, the parameter of the third side is defined. The diagonal electrode reactions correspond to concerted structural change and electron transfer.

As was shown earlier,[1] the cyclic voltammograms of **2** and **3** can be accounted for by two steps, each a concerted structural change and electron transfer. The first step is oxidation of N to $CR^{+\bullet}$ and the second oxidation of $CR^{+\bullet}$ to DC^{2+}. The parameter values that were found are given in Table 2.[1] As explained earlier, the fact that the values of the standard electron-transfer rate constants for **2** and **3** were much smaller than for **1** was attributed to postulated large structural changes accompanying the electron transfers of **2** and **3**. In other words, it was concluded that the inner reorganization energies for the electron-transfer reactions were large. However, as shown in the first part of this paper, the inner reorganization energies for the first step of oxidation of **2** and **3** are actually smaller than that of **1**. This result requires a reevaluation of the electrochemical data.

As shown above, the original conclusion[1] that substantial structural changes occur upon oxidation of **2** and **3** to their cation radicals and dications is supported by DFT calculations. The neutral compounds feature undistorted rings with the dimethylamino groups turned out of the plane. The cation radicals have two structures of comparable energy, one with the dimethylamino groups turned into the plane with resulting distortion of the ring and one a folded structure with a boat-shaped (central) ring. The dication structure is folded.

The alternative to a concerted structural change and electron transfer with a large inner reorganization energy is a two-step process in which electron transfer either precedes or follows the structural change which is a purely chemical process (conformation change or isomerization) that occurs in solution near the electrode. The first step of oxidation is then described by the square scheme on the lower right of Scheme 1. The second step appears in the upper left.

Simulations according to Scheme 1 were fit to the data for **2** and **3** as shown in Figures 5 and 6 and in the Supporting Information. The same parameter values were used to fit all scan rates (Table 2). There are a number of points to be made about the fits of simulation to experiment.

First, the voltammograms for both compounds can be adequately fit by Scheme 1 using the same parameter values for scan rates from 0.1 to 30 V/s. This shows that the earlier analysis[1] that assumed concerted structural change and electron transfer is not the only model that will account for the results. Second, the electron-transfer rate constants obtained by using Scheme 1 are not abnormally small, the smallest being 0.024 cm/s. This contrasts with values as small as 2.9×10^{-4} cm/s that were required in the earlier analysis,[1] which fact prompted the suggestion of large inner reorganization energies. Third, unlike the previous analysis where the required electron-transfer coefficients differed markedly from one-half (e.g., 0.20, 0.85, and 0.70),[1] the values were indistinguishable from one-half when evaluated according to Scheme 1. This results, of course, from the fact that the electron-transfer reactions in Scheme 1 are much more reversible so that the voltammograms are relatively insensitive to the value of the transfer coefficient. This is the most satisfying feature of the analysis according to Scheme 1 because it eliminates the suspicious values of transfer coefficients found earlier.[1]

Fourth, the actual magnitude of the rate constants in Table 2, both chemical and electrochemical, cannot be regarded as being quantitatively accurate. We simply report the set of values that we found by optimizing fits to the data. Still, it is useful to consider the qualitative features. For example, the first step of oxidation can in principle proceed by two routes, either electron transfer ($N \rightarrow N^{+\bullet} + e^-$) followed by structural change ($N^{+\bullet} \rightarrow CR^{+\bullet}$), an EC (electrochemical/chemical) path, or structural change ($N \rightarrow CR$) followed by electron transfer ($CR \rightarrow CR^{+\bullet} + e^-$), a CE (chemical/electrochemical) path. The optimized parameter values lead in turn to values of the kinetic parameters for EC and CE mechanisms[9,10] which show that the first step

TABLE 3: Definition of Parameters for Scheme 1[a]

chemical reactions (vertical)	electrode reactions (horizontal)	electrode reactions (diagonal)
$K_{CR/N} = c_{CR}/c_N = k_{N\rightarrow CR}/k_{CR\rightarrow N}$	$E°_{DC^{2+}/DC^+}$; $k_{s,DC^{2+}/DC^+}$; α_{DC^{2+}/DC^+}	$E°_{DC^{2+}/CR^+}$; $k_{s,DC^{2+}/CR^+}$; α_{DC^{2+}/CR^+}
$K_{CR^+/N^+} = c_{CR^+}/c_{N^+} = k_{N^+\rightarrow CR^+}/k_{CR^+\rightarrow N^+}$	$E°_{CR^{2+}/CR^+}$; $k_{s,CR^{2+}/CR^+}$; α_{CR^{2+}/CR^+}	$E°_{CR^+/N}$; $k_{s,CR^+/N}$; $\alpha_{CR^+/N}$
$K_{DC^+/CR^+} = c_{DC^+}/c_{CR^+} = k_{CR^+\rightarrow DC^+}/k_{DC^+\rightarrow CR^+}$	$E°_{CR^+/CR}$; $k_{s,CR^+/CR}$; $\alpha_{CR^+/CR}$	
$K_{DC^{2+}/CR^{2+}} = c_{DC^{2+}}/c_{CR^{2+}} = k_{CR^{2+}\rightarrow DC^{2+}}/k_{DC^{2+}\rightarrow CR^{2+}}$	$E°_{N^+/N}$; $k_{s,N^+/N}$; $\alpha_{N^+/N}$	

[a] $K_{j/k}$: equilibrium constant for k → j. c_j: equilibrium concentration of j. $k_{k\rightarrow j}$: rate constant for k → j. $E°_{k/j}$, $k_{s,k/j}$, $\alpha_{k/j}$: standard potential, standard electron-transfer rate constant, and electron-transfer coefficient for $k + e^- \rightleftharpoons j$.

occurs exclusively by the first path, electron transfer followed by structural change (EC). Similar qualitative analyses can be performed on the second oxidation step.

Fifth, the formal potentials and equilibrium constants from the present analysis may be combined to obtain the formal potentials for the two diagonal reactions in Scheme 1. These may be compared with the formal potentials evaluated earlier by assuming that each of these diagonal reactions was a concerted structural change and electron transfer[1] (Table 2). The agreement for the individual potentials is poor and in the direction in which analysis according to Scheme 1 predicts greater potential inversion. It has already been noted that it is difficult to determine the extent of inversion accurately when it is large, as it is for **2** and **3**.[11] However, the formal potential for the overall two-electron process, $E°_{overall}$, is in relatively good (<30 mV differences) agreement (Table 2).

Finally, it should be noted that our PES data speak only to the magnitude of the inner reorganization energy for the cation radicals of **1**−**3**, which is relevant to the first step of oxidation. We have no information about the inner reorganization energy for the cation radical/dication reaction which might actually be larger for **2** and **3** compared to **1**. Thus, we fit the data with the square scheme for the first electron transfer (lower right of Scheme 1) but a direct structural change/electron transfer for the second (diagonal reaction in upper left of Scheme 1. The agreement between simulations and experimental voltammograms was equally as good as that achieved with the entire Scheme 1.

4. Conclusion

The inner reorganization energy of the cation radical of **1** was determined by PES and shown to be 0.72 eV. The corresponding reorganization energies for **2** and **3** are smaller than that of **1**. This finding prompted a reinvestigation of the voltammetry of **2** and **3** which had previously been interpreted in terms of rather small electron-transfer rate constants that signified that the reorganization energies for **2** and **3** were larger, not smaller, than that of **1**. New voltammetric data were interpreted in terms of two-step electrode reactions, both electron transfer followed by structural change and structural change followed by electron transfer. Agreement of simulations with experiment was equally as good as in the previous work. This case is the first in which a non-electrochemical (PES) evaluation of reorganization energies has allowed discrimination between electrode reactions that are concerted electron transfer and structural change from those that are two-step electrode reactions with separate electron transfer and structural change.

Acknowledgment. The support of this research by the National Science Foundation, Grant CHE 0347471, is gratefully acknowledged.

Supporting Information Available: Comparison of simulations with experimental voltammograms for **2** and **3**. This material is available free of charge via the Internet at http://pubs.acs.org.

References and Notes

(1) Hu, K.; Evans, D. H. *J. Electroanal. Chem.* **1997**, *423*, 29−35.

(2) (a) Amashukeli, X.; Winkler, J. R.; Gray, H. B.; Gruhn, N. E.; Lichtenberger, D. L. *J. Phys. Chem. A* **2002**, *106*, 7593−7598. (b) Gruhn, N. E.; da Silva Filho, D. A.; Bill, T. G.; Malagoli, M.; Coropceanu, V.; Kahn, A.; Brédas, J.-L. *J. Am. Chem. Soc.* **2002**, *124*, 7918−7919. (c) Coropceanu, V.; Malagoli, M.; da Silva Filho, D. A.; Gruhn, N. E.; Bill, T. G.; Brédas, J.-L. *Phys. Rev. Lett.* **2002**, *89*, 275503−1. (d) Amashukeli, X.; Gruhn, N. E.; Lichtenberger, D. L.; Winkler, J. R.; Gray, H. B. *J. Am. Chem. Soc.* **2004**, *126*, 15566−15571.

(3) (a) Siegbahn, K.; Nordling, C.; Fahlman, A.; Nordberg, R.; Hamrin. *ESCA: Atomic, Molecular and Solid State Structure Studied by Means of Electron Spectroscopy*; Almqvist & Wiksells: Uppsala, 1967. (b) Lichtenberger, D. L.; Kellogg, G. E.; Kristofzski, J. G.; Page, D.; Turner, S.; Klinger, G.; Lorenzen. J. *Rev. Sci. Instrum.* **1986**, *57*, 2366. (c) Lichtenberger, D. L.; Copenhaver, A. S. *J. Electron Spectrosc. Relat. Phenom.* **1990**, *50*, 335−352. (d) Amashukeli, X.; Winkler, J. R.; Gray, H. B.; Gruhn, N. E.; Lichtenberger, D. L. *J. Phys. Chem. A* **2002**, *106*, 7593−7598.

(4) Hong, S. H.; Kraiya, C.; Lehmann, M. W.; Evans, D. H. *Anal. Chem.* **2000**, *72*, 454−458.

(5) Macías-Ruvalcaba, N. A.; Evans, D. H. *J. Phys. Chem. B* **2005**, *109*, 14642−14647.

(6) (a) Rudolph, M. *J. Electroanal. Chem.* **2003**, *543*, 23−29. (b) Rudolph, M. *J. Electroanal. Chem.* **2004**, *571*, 289−307. (c) Rudolph, M. *J. Electroanal. Chem.* **2003**, *558*, 171−176. (d) Rudolph, M. *J. Comput. Chem.* **2005**, *26*, 619−632**.** (e) Rudolph, M. *J. Comput. Chem.* **2005**, *26*, 633−641. (f) Rudolph, M. *J. Comput. Chem.* **2005**, *26*, 1193−1204.

(7) Frisch, M. J.; Trucks, G. W.; Schlegel, H. B.; Scuseria, G. E.; Robb, M. A.; Cheeseman, J. R.; Montgomery, J. A., Jr.; Vreven, T.; Kudin, K. N.; Burant, J. C.; Millam, J. M.; Iyengar, S. S.; Tomasi, J.; Barone, V.; Mennucci, B.; Cossi, M.; Scalmani, G.; Rega, N.; Petersson, G. A.; Nakatsuji, H.; Hada, M.; Ehara, M.; Toyota, K.; Fukuda, R.; Hasegawa, J.; Ishida, M.; Nakajima, T.; Honda, Y.; Kitao, O.; Nakai, H.; Klene, M.; Li, X.; Knox, J. E.; Hratchian, H. P.; Cross, J. B.; Adamo, C.; Jaramillo, J.; Gomperts, R.; Stratmann, R. E.; Yazyev, O.; Austin, A. J.; Cammi, R.; Pomelli, C.; Ochterski, J. W.; Ayala, P. Y.; Morokuma, K.; Voth, G. A.; Salvador, P.; Dannenberg, J. J.; Zakrzewski, V. G.; Dapprich, S.; Daniels, A. D.; Strain, M. C.; Farkas, O.; Malick, D. K.; Rabuck, A. D.; Raghavachari, K.; Foresman, J. B.; Ortiz, J. V.; Cui, Q.; Baboul, A. G.; Clifford, S.; Cioslowski, J.; Stefanov, B. B.; Liu, G.; Liashenko, A.; Piskorz, P.; Komaromi, I.; Martin, R. L.; Fox, D. J.; Keith, T.; Al-Laham, M. A.; Peng, C. Y.; Nanayakkara, A.; Challacombe, M.; Gill, P. M. W.; Johnson, B.; Chen, W.; Wong, M. W.; C. Gonzalez, C.; Pople, J. A. *Gaussian 03*, revision B.05; Gaussian, Inc.: Pittsburgh, PA, 2003.

(8) (a) Ballhausen, C. J. *Molecular Electronic Structures of Transition Metal Complexes*; McGraw-Hill: London, U.K., 1979; p 125. (b) Tutt, L.; Tannor, D.; Heller, E. J.; Zink, J. I. *Inorg. Chem.* **1982**, *21*, 3858−3859. (c) Barbara, P. F.; Meyer, T. J.; Ratner, M. A. *J. Phys. Chem.* **1996**, *10*, 0, 13148−13168. (d) Malagoli, M.; Coropceanu, V.; da Silva Filho, D. A.; Bredas, J. L. *J. Chem. Phys.* **2004**, *120*, 7490−7496.

(9) Nicholson, R. S.; Shain, I. *Anal. Chem.* **1964**, *36*, 706−723.

(10) Bard, A. J.; Faulkner, L. R. *Electrochemical Methods. Fundamentals and Applications*, 2nd ed.; Wiley: New York, 2001; Chapter 12.

(11) Kraiya, C.; Evans, D. H. *J. Electroanal. Chem.* **2004**, *565*, 29−35.